RESEARCH ARTICLE
SPACE PHYSICS: IONOSPHERIC PHYSICS

Earth and Planetary Physics
8: 408–414, 2024
doi: 10.26464/epp2024005

The nature of electron density enhancement over a wide altitude range during ionosphere heating experiments at EISCAT

Jun Wu[1]*, Jian Wu[1], Jie Feng[1,2], QingLiang Li[1], ShuJi Hao[1], ZhengWen Xu[1], HaiSheng Zhao[1], and YaBin Zhang[1]

[1]National Key Laboratory of Electromagnetic Environment, China Research Institute of Radio Wave Propagation, Beijing 102206, China;

[2]School of Physics, Xidian University, Xi'an 710071, China

Key Points:

- Whether the apparent enhancement in electron density observed over a wide altitude range actually corresponds to a true enhancement is still an open question.
- Observations at EISCAT during two heating experiments were analyzed by following the dispersion relation of ion acoustic waves.
- The apparent enhancement in electron density derived during the heating experiments may not be a true phenomenon.

Citation: Wu, J., Wu, J., Feng, J., Li, Q. L., Hao, S. J., Xu, Z. W., Zhao, H. S., and Zhang, Y. B. (2024). The nature of electron density enhancement over a wide altitude range during ionosphere heating experiments at EISCAT. *Earth Planet. Phys.*, *8*(2), 408–414. http://doi.org/10.26464/epp2024005

Abstract: During the course of ionospheric heating experiments, researchers at the European Incoherent Scatter Scientific Association (EISCAT) observed an apparent electron density enhancement. The enhancement extended over a wide range of altitudes, above the reflection altitude of the high-frequency pump wave. However, whether this enhancement actually corresponds to a true enhancement in electron density remains an open question. When the dispersion relation of ion acoustic waves is followed, the frequency ratio of the enhanced ion line to the background ion line suggests that the profile of the effective ion mass may have remained unchanged. Furthermore, the solar radio flux and ion drift velocity indicate no significant changes in the ion species and their densities. In conclusion, the electron density enhancement observed at EISCAT should not, in fact, be considered a true enhancement.

Keywords: incoherent scatter radar (ISR); ionospheric heating; electron density; ion acoustic wave

1. Introduction

In the F region of the ionosphere (altitudes >160 km), powerful high-frequency (HF) pump waves can regularly induce an appreciable change in electron density in the vicinity of the HF pump wave reflection altitude. Some studies in the past have typically observed such electron density modifications or theorized they exist. Utlaut and Violette (1972) inferred a ~7% decrease in the electron density from ionograms recorded at the Platteville Atmospheric Observatory, Colorado, USA (henceforth referred to as Platteville). Later, using the typical parameters at the Arecibo Observatory, Puerto Rico (henceforth referred to as Arecibo), and at Platteville, Meltz et al. (1974) suggested a theoretical decrease of ~3% in electron density 2 min after the onset of HF pumping. Experiments by Djuth et al. (1987) at Arecibo demonstrated that a decrease of ~10%–15% in the electron density was accompanied by a 1000–2000 K increase in the electron temperature. Duncan et al. (1988) reported the first thermally driven decrease of ~50% in electron density. However, observations at the European Incoherent Scatter Scientific Association (EISCAT) showed both an increase and a decrease in electron density in the vicinity of the reflection altitude of the HF pump wave, demonstrating disagreements with a time-dependent numerical model (Stocker et al., 1992). At the High-frequency Active Auroral Research Program (HAARP), Alaska, USA, Pedersen et al. (2010, 2011) observed a large enhancement in electron density at the altitude of ~220 km induced by the HF pump wave near the second electron gyroharmonic.

In recent years, an apparent enhancement in the electron density, induced by HF pump waves in the X mode (Senior et al., 2013) and O mode (Wu J et al., 2016, 2017), was observed over a wide range of altitudes above the pump wave reflection altitude. Senior et al. (2013) found that the shape of the enhanced ion line corresponded very closely to that of the ion line taken before the onset of pumping at the altitude of ~300 km, and that the frequency of the plasma line showed no appreciable change at the altitudes of ~321 and ~339 km. It was suggested that the apparent enhancement did not, in fact, correspond to a true enhancement in electron density. Instead, it corresponded to the enhanced ion line by some unknown mechanisms, which preferentially scatters the radar wave back along the magnetic field line. Rietveld and Senior (2020) proposed that medium- and large-scale field-aligned irregularities could refract the radar wave along the magnetic field. This could cause a strong radar backscatter, appearing in the

Correspondence to: J. Wu, wujun1969@163.com
Received 07 OCT 2023; Accepted 05 DEC 2023.
First Published online 15 JAN 2024.

observation as an enhanced electron density. However, Blagoveshchenskaya et al. (2022) claimed that this apparent enhancement did correspond to a true enhancement in electron density and might be due to increased ionization resulting from the flux of accelerated electrons. Indeed, the debate continues over the apparent or true nature of this enhancement in electron density, and conclusive proofs are still expected.

It is essential to confirm the apparent or true nature of the ionospheric electron density enhancement, on which the research path of physical mechanisms heavily depends. That is, if the apparent enhancement does, in fact, correspond to a true enhancement in electron density, the research of physical mechanisms will focus on the interaction between the HF pump wave and the ionospheric plasma; otherwise, it should focus on the scattering process of the radar wave. In this work, an alternative method, confirming the apparent or true nature of the ionospheric electron density enhancement, is presented, and two ionospheric heating experiments are examined.

2. Experiment and Data

At EISCAT, near Tromsø, Norway (69.58°N, 19.21°E), the heating facility can radiate an O/X mode HF pump wave in the frequency range of 4.0–8.0 MHz (Rietveld et al., 1993). It also hosts an ultra-high-frequency (UHF) incoherent scatter radar (ISR), operating at 930.0 MHz (Rishbeth and van Eyken, 1993). In this study, we examined two prior experiments involving the aforementioned heating facility and UHF ISR:

(1) The first experiment (henceforth referred to as Experiment 1) was conducted by Senior et al. (2013) on October 18, 2012, between 13:10 and 14:50 universal time (UT). The heating facility was operated at 7.953 MHz, pointing in the field-aligned direction (12° with the zenith, 186° with the azimuth) and with an effective radiated power of ~840.0 MW. The HF pump wave was modulated to stay on for 300 s, followed by a break of 300 s, with the polarization switching between the O and X modes on successive pulses, making an overall cycle of 1200 s. The radar beam began in the field-aligned direction for the first 120 s, followed by an alignment of 11° and 13° away from the zenith for 60 s each. Finally, the radar beam was returned to the field-aligned direction for 60 s before the HF pumping was turned off. The radar power was measured at ~1.5 MW, with the HF pumping on, and at ~1.6 MW, with the HF pumping off. The system temperature of the ISR remained at ~95 K throughout Experiment 1, and some deviations from 95 K appeared occasionally, of which the apparent enhancement in the electron density is independent temporally.

(2) The second experiment (henceforth referred to as Experiment 2) was conducted by Wu J et al. (2016, 2017) on March 11, 2014, between 12:30 and 14:30 UT. The heating facility was operated at frequencies in steps of 2.8 kHz from 6.7 MHz to 7.0 MHz. The effective radiated power had a range of 56.0–78.0 MW. The O mode HF pump wave was modulated to stay on for 18 min and then, off for 12 min. The radar beam and HF pump beam stayed in the field-aligned direction throughout the experiment. The radar power was measured at ~1.4 MW, with the pumping on and at ~1.5 MW, with the HF pumping off. Throughout Experiment 2, the system temperature of the ISR was similar to that in Experiment 1 and had a value of ~100 K.

In addition, Senior et al. (2013) and Wu J et al. (2016, 2017) gave a detailed description of the two experiments, where more experimental information is available. To allow ion line smoothing, the ISR data in this study were analyzed by using an integration time of 60 s.

Figure 1 displays the mean electron density N_e, mean electron temperature T_e, mean ratio of electron temperature to ion temperature $\frac{T_e}{T_i}$, and mean ion drift velocity v_D. As the regular ISR observations in ionosphere heating experiments, some significant increases of ~50% and ~19% in N_e, ~60% and ~30% in T_e, and ~130% and ~30% in $\frac{T_e}{T_i}$ can be seen in the narrow altitude range of ~200–300 km for Experiments 1 and 2, respectively. Here, the increases in T_e and $\frac{T_e}{T_i}$ were attributed to (i) the weak leakage of the X mode pump wave into the O mode by Senior et al. (2013), and (ii) the upper hybrid resonance close to the reflection altitude of the HF pump wave by Wu J et al. (2017). And the increase in N_e was not a true enhancement in electron density but was due to the enhanced ion lines by the parametric decay instability near the reflection altitude of the HF pump wave (Robinson, 1989). In addition, because of the weaker ISR echo from a scattering volume above the altitude of ~500 km, the smaller signal-to-noise ratio (SNR) leads to contaminated profiles of T_e, $\frac{T_e}{T_i}$, and v_D above an altitude of ~500 km. Moreover, because N_e is dependent on only the power of the ion lines, the profile of N_e is not contaminated above the altitude of ~500 km. Additionally, no evidence exists of a significant change in v_D throughout both experiments, that is, v_D remained at ~10 m/s above the altitude of ~350 km and at ~20 m/s below the altitude of ~350 km. This result implies that v_D was not disturbed by the HF pump wave and that the drift of ionospheric plasma was not active in the geomagnetic field-aligned direction.

In particular, in both cases, unexpected enhancements of ~43% and ~30% in N_e were observed above the altitude of ~300 km until the altitude limit of the radar measurement. This result was consistent with a clear enhancement in the ion lines within the altitude range of 245–486 km, as illustrated in Figure 2.

Figure 2 illustrates examples of ion lines in the altitude range of ~245–500 km for both experiments. It is evident that in both cases, when the pumping is on, the ion lines at ~9.5 kHz are significantly enhanced in intensity. According to the standard analysis of incoherent scatter, this observation would indicate that the profile of electron density N_e is modified by the HF pumping. Moreover, the intensity of the ion lines below an altitude of ~314 km are an order of magnitude more intense than the intensity above the altitude of ~314 km, that is, depending on the N_e profile and the radar echo scattered from the scattering volume.

To summarize, as observed in Figures 1 and 2, a notable enhancement is seen in N_e and the ion lines in the altitude range of ~300–500 km when the HF pumping is on. It should be emphasized that the apparent enhancements are unexpected because (i) the HF pump wave should be reflected at its reflection altitude (i.e., the ionosphere above the reflection altitude should not be

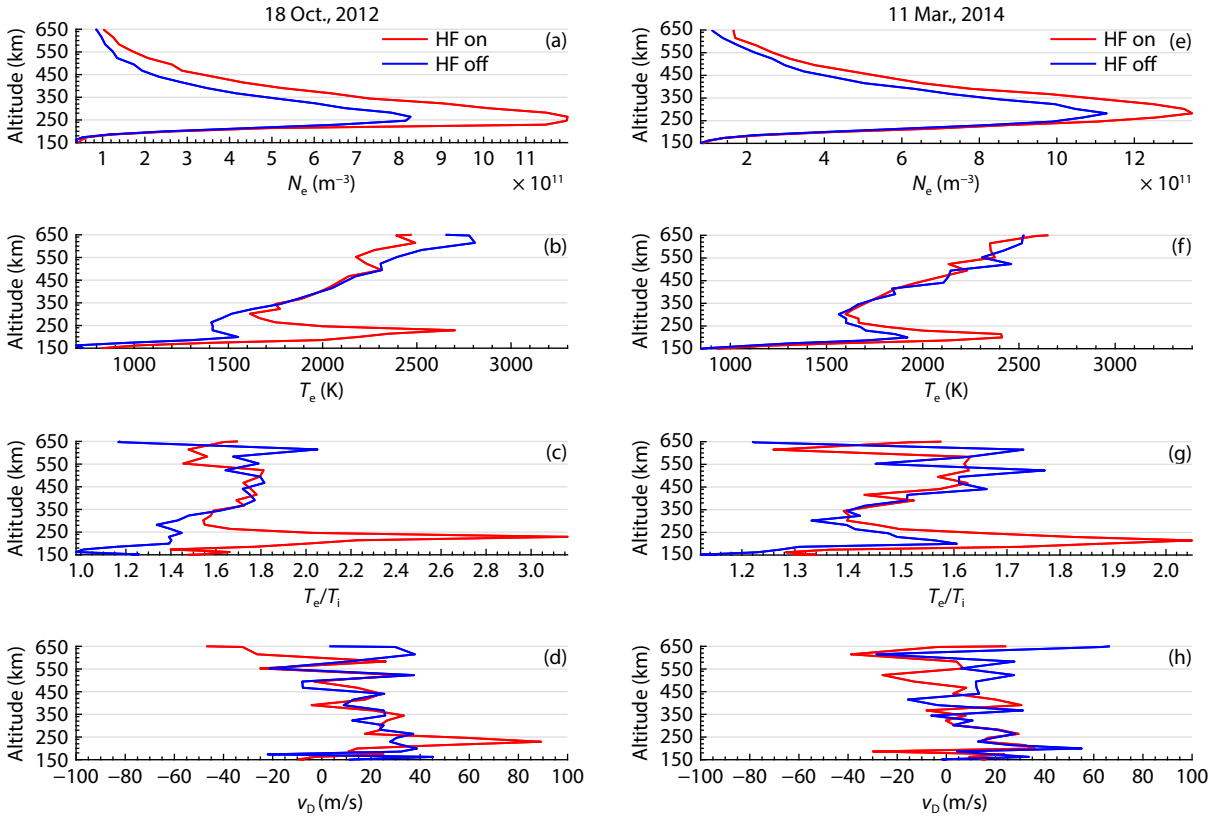

Figure 1. (a) Mean electron density; (b) mean electron temperature; (c) mean ratio of electron temperature to ion temperature; and (d) mean ion drift velocity measured in Experiment 1. Each enhanced (red) or background (blue) value is the mean of the integration of the X mode pump wave, over the final 60 s of the on/off period, for five cycles. Subplots (e), (f), (g), and (h) correspond to (a), (b), (c), and (d), respectively, for Experiment 2, and the description follows that of Experiment 1 but measured over only three on/off cycles. The values were obtained by using the Grand Unified Incoherent Scatter Design and Analysis Package (GUISDAP; Lehtinen and Huuskonen, 1996).

disturbed by the pump wave; Robinson, 1989), and (ii) only N_e was enhanced, whereas other parameters remained unchanged.

3. Discussion

Because the parameters and ion lines described in Section 2 were obtained by using the GUISDAP and RTG, which are based on the standard incoherent scatter analysis, a Maxwellian plasma is assumed here. In addition, considering the reflection of the HF pump wave near the altitude of 240 km and the unchanged profiles of T_e, $\frac{T_e}{T_i}$, and v_D in the altitude range of ~300–500 km, one should be confident in the Maxwellian assumption.

For $\frac{T_e}{T_i} \leqslant 4$, the incoherent backscattered power P_r can be expressed as (Evans, 1969; Djuth et al., 1987; Duncan et al., 1988)

$$P_r \propto N_e \sigma_e \left(1 + \frac{T_e}{T_i}\right)^{-1}, \tag{1}$$

where σ_e is the Thomson cross section for electrons. In Figures 1c and 1g, $\frac{T_e}{T_i}$ shows no appreciable change in the altitude range of ~300–500 km in either experiment, implying that the ion lines in Figure 2 were enhanced only as a result of the enhanced N_e, as indicated by Equation (1). On the other hand, N_e is enhanced solely because of the enhanced ion line, as indicated by the standard analysis of incoherent scatter. Thus, the enhanced N_e is equivalent to the enhanced ion line (i.e., a closed relationship exists between the enhanced N_e and the enhanced ion line), which satisfies the incoherent scatter theory. Obviously, for confirming the apparent or true nature of the enhanced N_e, examining the ion line intensity becomes invalid. Hence, instead of the ion line intensity, we will examine the ion line frequency.

For the quasi-neutral F region of the ionosphere, an ion acoustic wave should satisfy (Robinson, 1989; Kohl et al., 1993; Alcaydé, 1995)

$$\omega_i^2 = K_B \frac{\gamma T_i + T_e}{M_i} k_i^2, \tag{2}$$

where ω_i, k_i, γ, K_B, and M_i denote the angular frequency, wave number, adiabatic index, Boltzmann constant, and effective ion mass, respectively. In the case of backscatter, the ISR can observe only an ion acoustic wave satisfying the Bragg condition $k_i = 2k_r$, where k_r denotes the wave number of the ISR and has a value of 19.5 m^{-1} for the UHF ISR at EISCAT. This result implies that all the ion lines observed in Experiments 1 and 2 (Figure 2) satisfy the Bragg condition. In other words, $k_i = 39$ m^{-1} is a constant for all the ion lines examined, although those ion acoustic waves within a small range of $2k_r$ may also contribute (Hagfors, 2003). Moreover, in both experiments, the profiles of T_e and $\frac{T_e}{T_i}$ are independent of the HF pumping in the altitude range of ~300–500 km

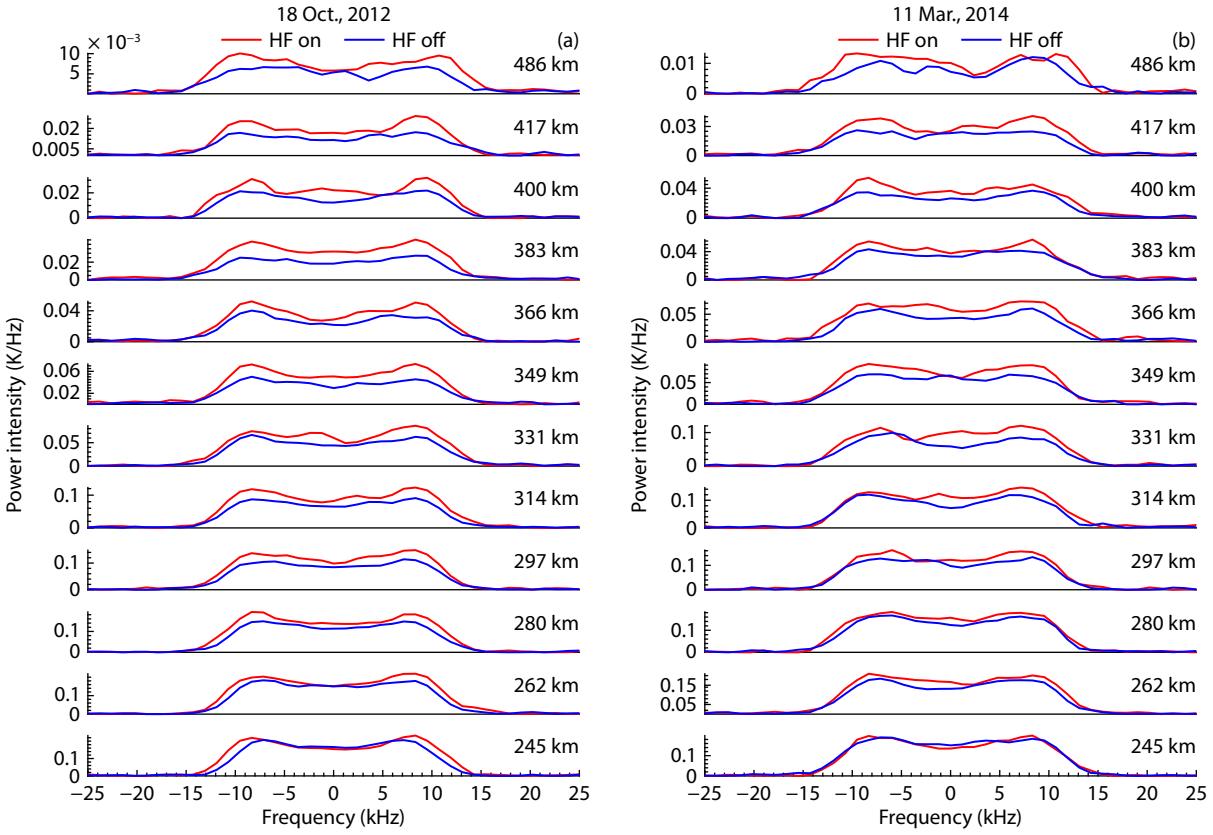

Figure 2. (a) Examples of ion lines measured in Experiment 1; (b) examples of ion lines measured in Experiment 2. The ion lines were obtained by using the EISCAT Real Time Graphic (RTG) package. The ion lines above the altitude of ~500 km are not shown because of the smaller SNR of the ISR echo. Additionally, the ion line measurement follows the same method as in Figure 1.

(Figures 1b, 1c, 1f, and 1g); that is, although some natural variability exists in the profiles of T_e and $\frac{T_e}{T_i}$, they can still be considered to have a quasi-constant profile in the altitude range of interest. In other words, it can reasonably be considered that the profiles of T_e and $\frac{T_e}{T_i}$ remained unchanged in the altitude range of ~300–500 km throughout both experiments. Thus, the straightforward relation between ω_i and M_i is obtained as

$$\omega_i^2 = \frac{a}{M_i}, \tag{3}$$

where $a = \left(\frac{\gamma}{T_e/T_i} + 1\right) K_B T_e k_i^2$ is a quasi-constant profile in the altitude range of interest.

Equation (3) indicates that, throughout the experiments, the profile of ω_i is dependent on that of M_i, namely, the change in ω_i should be dependent on the change in M_i. Figure 3 demonstrates the ratio of the enhanced ion line angular frequency ω_i^{on} to the background ion line angular frequency ω_i^{off} as a function of altitude. As shown in Figure 3, note that the SNR of this ratio in Experiment 1 is obviously larger than that in Experiment 2, and especially that the SNR around ~360–380 km in Experiment 1 and around ~300–370 km in Experiment 2 are obviously small. This may be the result of (i) the higher number of observation cycles in Experiment 1 (five cycles) compared with Experiment 2 (three cycles); (ii) the higher radar power with pumping on in Experiment 1 compared with Experiment 2 (i.e., the radar echo may have been more intense during Experiment 1); (iii) the lower system temperature of the radar in Experiment 1 (~95 K) compared with Experiment 2 (~100 K); and (iv) a data processing error by the GUISDAP.

From Figure 3a, we can observe that $\frac{\omega_i^{on}}{\omega_i^{off}}$ has a mean of ~1.03 in the altitude range of ~270–450 km, implying that the ion line frequency was not significantly changed by the HF pumping in Experiment 1. Thus, following Equation (3), $\frac{M_i^{off}}{M_i^{on}}$ has a mean of ~1.06 in the altitude range of ~270–450 km, where M_i^{on} denotes the effective ion mass with the pumping on and M_i^{off} denotes the effective ion mass with the pumping off. Considering the aforementioned error of the SNR, this may imply that M_i was not significantly changed by the HF pumping in the altitude range of ~270–450 km. However, below the altitude of ~270 km, $\frac{\omega_i^{on}}{\omega_i^{off}}$ has a mean of ~1.2. This change can be attributed to the natural ion acoustic waves close to ω_i^{on}. Here, to distinguish them from the HF enhanced ion acoustic waves by the parametric decay instability, the natural ion acoustic waves denote the waves unaffected by the HF pump wave. The natural ion acoustic wave covers a wide frequency spectrum owing to the highly varied ion mass distribution in the ionosphere, in which some of the higher frequencies could satisfy the Bragg condition owing to the enhanced T_e as indicated by Equation (2) . In other words, following Equation (2) and considering a constant M_i, when T_e becomes higher, the ion

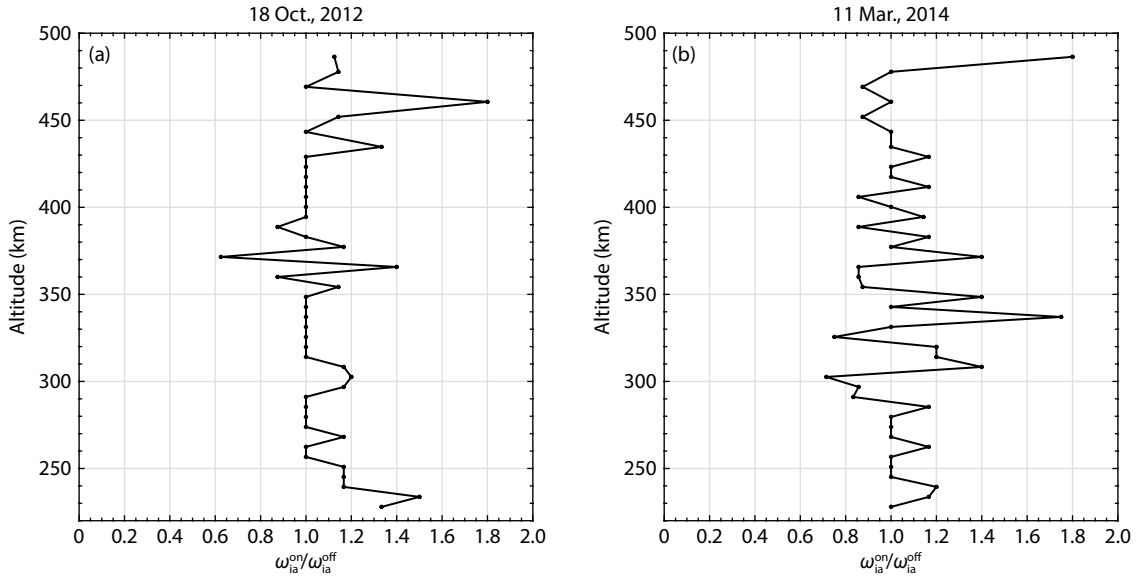

Figure 3. (a) Ratio of the enhanced ion line frequency to the background ion line frequency, measured in Experiment 1; (b) same ratio as in (a) for Experiment 2, where the frequency is the value corresponding to the maximum intensity of the right shoulder of the ion line.

acoustic waves at the higher frequencies will be observed. Thus, below the altitude of ~270 km, the enhanced T_e leads to $\frac{\omega_i^{on}}{\omega_i^{off}} > 1$, for instance, at the altitude of ~230 km, the enhanced T_e of ~2700 K (the ratio of the enhanced electron temperature to the background temperature $\frac{T_e^{on}}{T_e^{off}} \approx 2$) in Figure 1b leads to $\frac{\omega_i^{on}}{\omega_i^{off}} \approx 1.50$ in Figure 3a . The measurement error, resulting from the small SNR, may lead to the increased frequency ratio mean value of ~1.24 above the altitude of ~450 km. Indeed, Equation (1) indicates that P_r must be reduced above the altitude of ~450 km because of the decreasing N_e and increasing $\frac{T_e}{T_i}$, as shown in Figure 1. Similarly, the aforementioned behavior holds true for Experiment 2, namely, $\frac{\omega_i^{on}}{\omega_i^{off}}$ has a mean of ~1.04 in the altitude range of ~270–450 km, ~1.05 below the altitude of ~270 km, and ~1.4 above the altitude of ~450 km, as shown in Figure 3b. It is important to note that in the altitude range of ~270–450 km, although the intensity of the ion lines is enhanced when the HF pumping is on, their frequency remains unchanged. Following Equation (3), this result implies that the M_i profile may remain unchanged in the altitude range of ~270–450 km.

Now, M_i can be expressed as

$$M_i = \frac{1}{N_e}\sum_i N_i m_i, \tag{4}$$

where N_i and m_i denote the density and mass of ion species, respectively. The quantity $N_i m_i$ is dependent on the incident radiation and the atmospheric composition, regardless of the corpuscular ionization, which may be significant in the nighttime ionosphere (Rishbeth and Garriott, 1969). With a constant profile of atmospheric composition, a strong incident radiation could lead to an increase in N_i. As indices of solar activity (Nicolet and Bossy, 1985), solar radio fluxes (SRFs) were measured at 245.0, 410.0, 610.0, 1415.0, 2695.0, 4995.0, 8800.0, and 15,400.0 MHz, as shown in Figure 4. With the exception at 610.0 MHz, the SRFs do not demonstrate a significant and systematic variation in intensity during either experiment. At 610.0 MHz, the intensity of the SRF varied between ~10,000 solar flux units (SFU) in Experiment 1 and ~140,000 SFU in Experiment 2. Obviously, the SRFs do not temporally synchronize with the enhanced N_e. In addition, the HF pump wave was reflected at the altitude of ~240 km for Experiment 1 and at ~230 km for Experiment 2. Thus, in both experiments, it is reasonable to assume that the incident radiation does not have a significant impact on N_i.

Moreover, an analysis of the vertical drift of plasma in both experiments shows that $v_D \approx 0$, indicating no active drift of plasma along the magnetic field lines and suggesting no induced change in the ion species. Nevertheless, a further examination of the change in ion species is needed. The ionosphere is mainly composed of hydrogen ions H^+, helium ions He^+, nitrogen ions N^+, atomic oxygen ions O^+, molecular oxygen ions O_2^+, and nitric oxide ions NO^+ in the altitude range of interest (Robinson, 1989). The frequency of the ion acoustic wave corresponding to H^+ is $\frac{k_r}{2\pi}\sqrt{\gamma\frac{K_B T_e}{m_{iH^+}}} \approx 43.7$ kHz, where $k_r = 39\ m^{-1}$ for the UHF radar, γ denotes the adiabatic index, K_B denotes the Boltzmann constant, m_{iH^+} denotes the mass of H^+, and T_e is ~2000 K, as given in Figure 1. This result indicates that the frequency of the ion acoustic wave corresponding to H^+ does not lie in the ion line channel of [–40 kHz, 40 kHz] of the UHF ISR at EISCAT, implying that the ion acoustic wave corresponding to H^+ cannot be collected by the UHF ISR. Similarly, the frequency of the ion acoustic wave corresponding to He^+ is ~22 kHz, which deviates significantly from the ~9.5 kHz shown in Figure 2. The frequencies of the ion acoustic waves corresponding to N^+, O^+, O_2^+, and NO^+, respectively, are ~11.5 kHz, ~10.5 kHz, ~7.8 kHz, and ~8 kHz, all of which may contribute to the ion lines at ~9.5 kHz shown in Figure 2. Considering that the frequencies of ion lines show no significant

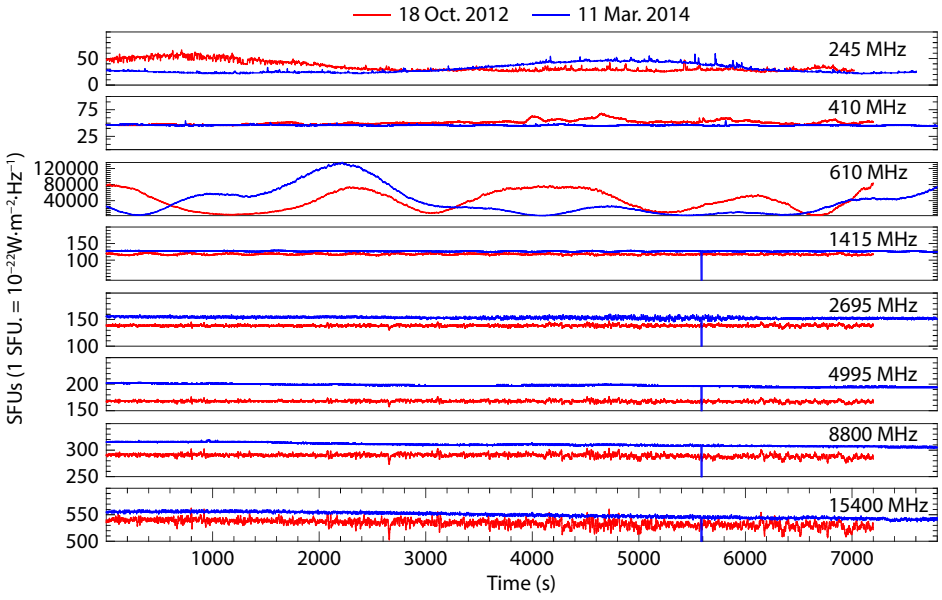

Figure 4. Solar radio fluxes above the baseline as recorded at the Radio Solar Telescope Network radio observatory in San Vito, Italy. The abscissa origin denotes 13:00 UT on October 18, 2012 (Experiment 1) and 12:20 UT on March 11, 2014 (Experiment 2).

change in Figure 2, the ion species of N^+, O^+, O_2^+, and NO^+ may not have been modified in the altitude range of interest. Both these analyses strongly imply that no modification has occurred in the ion species.

As a result, a straightforward relation between M_i and N_e can be obtained as

$$M_i = \frac{\beta}{N_e}, \tag{5}$$

where $\beta = \sum_i N_i m_i$ is a quasi-constant profile. Equation (5) indicates that, during the course of both experiments, because no modifications occurred in M_i, N_e must also not have been enhanced by the HF pumping in the altitude range of ~270–450 km.

4. Summary

With regard to the apparent enhancement in electron density over a wide altitude range during the ionospheric heating experiments, the observations at EISCAT were investigated by following the dispersion relation of ion acoustic waves.

Our investigation showed no significant modifications in the ion line frequency and the electron temperature in the altitude range of interest, which strongly implies that the profile of the effective ion mass must remain unchanged. Moreover, the incident radiation and the ion drift velocity indicate that the ion species and their densities must not have been modified. With the assumption of quasi-neutrality, it can be reasonably concluded that the apparent electron density enhancement does not, in fact, correspond to a true enhancement in electron density, which preferentially supports the suggestion by Senior et al. (2013) and the proposal for a physical mechanism by Rietveld and Senior (2020).

Acknowledgments

The authors thank the editor and anonymous reviewers for their constructive and helpful comments, UK colleagues for their significant efforts in the experiment, the National Centers for Environmental Information for providing the SRF data, and Ingemar Haggstrom for the fruitful discussion about EISCAT data. EISCAT is an international association supported by research organizations in China (CRIRP), Finland (SA), Japan (NIPR and STEL), Norway (NFR), Sweden (VR), and the United Kingdom (NERC). ZhengWen Xu is supported by the Taishan Scholars Project of Shandong Province (Grant No. ts20190968). This work was supported by the foundation of National Key Laboratory of Electromagnetic Environment (Grant No. 6142403230303).

Open Research

Data Availability Statement: The ISR and SRF data, respectively, are available free of charge for public download at https://portal.eiscat.se/schedule/ and https://www.ngdc.noaa.gov/stp/space-weather/solar-data/solar-features/solar-radio/rstn-1-second/.

References

Alcaydé, D. (1995). Incoherent scatter, theory, practice and science. In *Proceedings of the 7th EISCAT Scientific Workshop* (pp. 33–66). Cargèse, Corsica: EISCAT Scientific Association.

Blagoveshchenskaya, N. F., Borisova, T. D., Kalishin, A. S., Egorov, I. M., and Zagorskiy, G. A. (2022). Disturbances of electron density in the high latitude upper (F-region) ionosphere induced by X-mode HF pump waves from EISCAT UHF radar observations. *Arct. Antarct. Res.*, *68*(3), 248–257. https://doi.org/10.30758/0555-2648-2022-68-3-248-257

Djuth, F. T., Thidé, B., Ierkic, H. M., and Sulzer, M. P. (1987). Large F-region electron-temperature enhancements generated by high-power HF radio waves. *Geophys. Res. Lett.*, *14*(9), 953–956. https://doi.org/10.1029/GL014i009p00953

Duncan, L. M., Sheerin, J. P., and Behnke, R. A. (1988). Observations of ionospheric cavities generated by high-power radio waves. *Phys. Rev. Lett.*, *61*(2), 239–242. https://doi.org/10.1103/PhysRevLett.61.239

Evans, J. V. (1969). Theory and practice of ionosphere study by Thomson scatter radar. *Proc. IEEE*, *57*(4), 496–530. https://doi.org/10.1109/PROC.1969.7005

Hagfors T. (2003). Basic physics of incoherent scatter. EISCAT Summer School 2003, SRI, Menlo Park, California, August 2003.

Kohl, H., Kopka, H., Stubbe, P., and Rietveld, M. T. (1993). Introduction to ionospheric heating experiments at Tromsø—II. Scientific problems. *J. Atmos. Terr. Phys.*, *55*(4-5), 601–613. https://doi.org/10.1016/0021-9169(93)90008-M

Lehtinen, M. S., and Huuskonen, A. (1996). General incoherent scatter analysis and GUISDAP. *J. Atmos. Terr. Phys.*, *58*(1-4), 435–452. https://doi.org/10.1016/0021-9169(95)00047-X

Meltz, G., Holway L. H., Jr., and Tomljanovich, N. M. (1974). Ionospheric heating by powerful radio waves. *Radio Sci.*, *9*(11), 1049–1063. https://doi.org/10.1029/RS009i011p01049

Nicolet, M., and Bossy, L. (1985). Solar radio fluxes as indices of solar activity. *Planet. Space Sci.*, *33*(5), 507–555. https://doi.org/10.1016/0032-0633(85)90096-0

Pedersen, T., Gustavsson, B., Mishin, E., Kendall, E., Mills, T., Carlson, H. C., and Snyder, A. L. (2010). Creation of artificial ionospheric layers using high-power HF waves. *Geophys. Res. Lett.*, *37*(2), L02106. https://doi.org/10.1029/2009GL041895

Pedersen, T., McCarrick, M., Reinisch, B., Watkins, B., Hamel, R., and Paznukhov, V. (2011). Production of artificial ionospheric layers by frequency sweeping near the 2nd gyroharmonic. *Ann. Geophys.*, *29*(1), 47–51. https://doi.org/10.5194/angeo-29-47-2011

Rietveld, M. T., Kohl, H., Kopka, H., and Stubbe, P. (1993). Introduction to ionospheric heating at Tromsø—I. Experimental overview. *J. Atmos. Terr. Phys.*, *55*(4-5), 577–599. https://doi.org/10.1016/0021-9169(93)90007-L

Rietveld, M. T., and Senior, A. (2020). Ducting of incoherent scatter radar waves by field-aligned irregularities. *Ann. Geophys.*, *38*(5), 1101–1113. https://doi.org/10.5194/angeo-38-1101-2020

Rishbeth, H., and Garriott, O., K. (1969). *Introduction to Ionospheric Physics*. New York: Academic Press.

Rishbeth, H., and Van Eyken, A. P. (1993). EISCAT: Early history and the first ten years of operation. *J. Atmos. Terr. Phys.*, *55*(4-5), 525–542. https://doi.org/10.1016/0021-9169(93)90002-G

Robinson, T. R. (1989). The heating of the high lattitude ionosphere by high power radio waves. *Phys. Rep.*, *179*(2-3), 79–209. https://doi.org/10.1016/0370-1573(89)90005-7

Senior, A., Rietveld, M. T., Häggström, I., and Kosch, M. J. (2013). Radio-induced incoherent scatter ion line enhancements with wide altitude extents in the high-latitude ionosphere. *Geophys. Res. Lett.*, *40*(9), 1669–1674. https://doi.org/10.1002/grl.50272

Stocker, A. J., Honary, F., Robinson, T. R., Jones, T. B., Stubbe, P., and Kopka, H. (1992). EISCAT observations of large scale electron temperature and electron density perturbations caused by high power HF radio waves. *J. Atmos. Terr. Phys.*, *54*(11-12), 1555–1572. https://doi.org/10.1016/0021-9169(92)90163-F

Utlaut, W. F., and Violette, E. J. (1972). Further ionosonde observations of ionospheric modification by a high-powered HF transmitter. *J. Geophys. Res.*, *77*(34), 6804–6818. https://doi.org/10.1029/JA077i034p06804

Wu, J., Wu, J., and Xu, Z. W. (2016). Results of ionospheric heating experiments involving an enhancement in electron density in the high latitude ionosphere. *Plasma Sci. Technol.*, *18*(9), 890. https://doi.org/10.1088/1009-0630/18/9/03

Wu, J., Wu, J., Rietveld, M. T., Haggstrom, I., Zhao, H. S., and Xu, Z. W. (2017). The behavior of electron density and temperature during ionospheric heating near the fifth electron gyrofrequency. *J. Geophys. Res.: Space Phys.*, *122*(1), 1277–1295. https://doi.org/10.1002/2016JA023121